A NOVEL EXTREMUM SEEKING SCHEME FOR CLOSED-LOOP JET CONTROL

Fan D W, Wu Z*, Cao H L, Yang H, Zhou Y
Institute for Turbulence-Noise-Vibration Interactions and Control
Shenzhen Graduate School, Harbin Institute of Technology, Shenzhen, China
*Corresponding author: wuzhiabcd@163.com

ABSTRACT

Jet control is of great interest to a wide range of industrial and environmental applications. This work presents an investigation on the closed-loop control of a turbulent round jet for enhancing the jet mixing. The Reynolds number Re_D range is 7333 to 9600 based on the jet exit diameter D and the exit velocity U_e. A single unsteady minijet is deployed upstream of the jet exit, which is produced through the on-off state of an electromagnetic valve. The open-loop control is investigated first. It has been found that, given the duty cycle a and volumetric flow rate ratio C_m of the minijet to that of the main jet, the decay rate K of jet centerline mean-velocity exhibits a maximum at the frequency ratio $f_e/f_0 \approx 0.5$, where f_e and f_0 are the excitation frequency of the minijet and the preferred mode frequency of the natural main jet, respectively. A novel extremum seeking closed-loop scheme is then investigated, with a view to achieving the optimal jet control performance automatically. The feedback signal is provided by the jet decay rate K_1 of jet centerline running-mean velocity measured by a hot-wire, based on which the output voltage signal controls the frequency of the electromagnetic valve. Comparing with classical extremum seeking schemes, the present scheme introduces an input estimation error to adjust adaptively the excitation frequency, thus reducing greatly the steady-state oscillation and hence enhancing K_1. Furthermore, this scheme is robust when Re_D and initial f_e are separately changed.

INTRODUCTION

As one of typical basic shear flows, jet mixing is widely seen in engineering, e.g. in aero and automobile engines, combustion, heat transfer and chemical reactors. Naturally, jet mixing enhancement has received large numbers of attention in literature.

Passive techniques were firstly applied to enhance jet mixing, such as deploying tabs [1] and using noncircular nozzles at the nozzle exit [2]. Azimuthal non-uniformities at the jet exit may have a dramatic impact on the evolution of shear layers, because the three-dimensional jet development is particularly sensitive to initial conditions. Noncircular jets are naturally more unstable than the circular counterpart [3], which exhibit shorter potential core length due to faster velocity decay. In practice, the operation state of the jet often vary, e.g., burners used in the process industries. The operation state of the actuator is difficult to change arbitrarily by passive control according to the variation of initial conditions. In order to overcome the drawback of the passive control, some active control techniques were proposed, including acoustic excitation [4], synthetic jet actuators [5] and plasma actuators [6]. For some applications, the pulsed or unsteady jet may be used to improve the actuator efficiency [7]. Zhou et al. [8] use unsteady minijets to enhance jet mixing of a round jet, finding the quasi-steady longitudinal counter-rotating vortex pairs induced by the unsteady minijets could enhance the centreline velocity decay rate. However, most jet mixing studies were performed in open-loop. Thus, it is inefficient to remove perturbations induced by external sources, e.g., Reynolds number change. The sensor-feedback or closed-loop may treat effectively the random-phase problem in turbulence dynamics [9] and allow flexibly controlled jet mixing [10]. The latter is important since the optimal control configuration of jet mixing varies with the operating conditions such as Mach number and temperature ratio.

The well-known extremum seeking is a model-free closed-loop control schemes. The objective of these controllers is to maximize or minimize the output of a flow system via online optimization of actuator parameters. When the steady-state input-output map has a well-defined extremum, the extremum seeking controller can be implemented to achieve the optimal control performance [11]. When the control performance is characterized by a saturated plateau in the input-output map, the slope-seeking controller was more suitable than the extremum seeking controller [12]. Wang et al. [13] propose a novel extremum seeking scheme to eliminate the steady-state oscillation by using a variable perturbation amplitude in the extremum seeking scheme [13]. The simulation results indicate this scheme could greatly improve the dynamic and static performance of the extremum seeking scheme.

This work aims to study a novel extremum seeking control system for jet flow control, where the jet centreline velocity decay rate K and the excitation frequency of minijet f_e are used as the feedback signal and the control signal, respectively. The novel extremum seeking is investigated and compared with the classical extremum seeking in the steady-state error of K and f_e. The robustness at different Reynolds number Re_D (range from 7333 to 9600), and adaptability at different initial excitation frequency $f_{e,i}$ of the novel control system are also investigated.

NOMENCLATURE

a	[Hz]	Amplitude of sinusoidal perturbation signal
C_m	[-]	Volumetric flow rate ratio of minijet to that of the main jet
D	[mm]	Exit diameter of the nozzle extension
f_e	[Hz]	Excitation frequency of minijet
$f_{e,i}$	[Hz]	Initial excitation frequency
$f_{e,optimal}$	[Hz]	Optimal value of excitation frequency
f_0	[Hz]	Preferred-mode frequency in the uncontrolled jet with C_m = 0 and f_e = 0
f_p	[Hz]	Perturbation frequency
K	[-]	Jet centerline velocity decay rate
k	[-]	Gain
Re	[-]	Reynolds number
U	[m/s]	Streamwise velocity component along x-axis of Cartesian coordinates
U_e	[m/s]	Jet centerline velocity at the exit of the nozzle extension
x		x axis of Cartesian coordinates
y		y axis of Cartesian coordinates
z		z axis of Cartesian coordinates
HP		High-Pass filter
LP		Low-Pass filter
r	[-]	The gain for adjusting the amplitude a of the novel extremum seeking scheme
F		A function of <K> and f_e
ϕ		Phase
Special characters		
$\langle\ \rangle$	[-]	Averaged quantity using 0.4-sec-long running window
Δ	[-]	Correction term
Subscripts		
e		Exit of the nozzle extension
c		Jet centerline
$3D$		x = 3D

JET FACILITY AND ACTUATOR SYSTEM

All experiments were performed in a round air facility. The jet facility is composed of main-jet and minijet assemblies. The minijet includes a stationary disk and an electromagnetic valve. Figure 1 shows the schematic diagram of the jet facility. Compressed air pass through a tube, a plenum chamber, a 300-mm-long diffuser of 15° in half angle, two fine screens (7mesh/cm) and a cylindrical settling chamber of 400 mm in length and 114 mm in inner diameter. The nozzle contraction followed a contour specified by equation $R = 57-47\sin^{1.5}(90-9x/8)$, as used by [14]. The contraction ratio was 32.5 with an exit diameter D of 20 mm. The nozzle was extended by a 47-mm-long smooth tube of the same diameter D. The exit Reynolds number $Re_D = U_eD/\nu$ of the main jet was fixed to 8000 mostly, where U_e (6 m/s) is the jet centerline velocity measured at the exit of the nozzle extension and ν is the kinematic viscosity.

Figure 1(b) shows the minijet assembly. A new unsteady minijet actuator is applied. The stationary disk was drilled with one orifice of 4 mm in diameter along the horizontal direction. The orifice was connected via short plastic hose to a constant-pressure chamber. The unsteady minijet actuator is actually controlled by an electromagnetic valve (Koganei K2-100SF-09-LL) with maximum frequency of 1 kHz. The contraction nozzle was drilled with one orifice of 1 mm in diameter, and located at 17 mm upstream of the extension exit. The electromagnetic is driven by the modified voltage signal (0-5V square wave signal) that may act to adjust the frequency of air injection with a maximum of 450 Hz, exceeding $3f_0$ as is evident in Figure 2(a, b), where f_0 is the preferred mode frequency of the natural main jet. The volumetric flow rates of both main jet and minijet were changed and measured respectively by two flow meters, whose experimental uncertainty was no more than 1%. The volumetric flow rate required by one minijet was further quantified using a dimensionless volumetric flow rate ratio C_m of the minijet to that of the main jet.

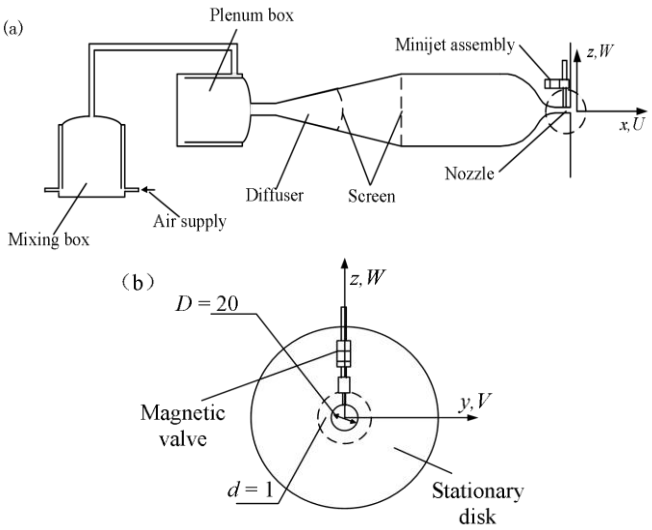

Figure 1 Schematic of experimental setup: (a) main-jet assembly; (b) minijet assembly.

The coordinate system is defined such that its origin is at the center of the nozzle extension exit, with the x axis along the streamwise direction, the z axis along the radial minijet and the y axis along the direction nomal to (x, z) plane, following the right-hand system. The (x, z) and (x, y) planes are referred to as the injection and non-injection planes, respectively. Following reference [8], the jet centerline decay rate K is used to evaluate main jet mixing, given by $K = \left(\overline{U_e} - \overline{U_{5D}}\right)/\overline{U_e}$, where $\overline{U_e}$ and $\overline{U_{5D}}$ are the mean jet centerline velocity at x/D = 0.05 and at x/D = 5, respectively.

HOTWIRE MEASUREMENTS AND CLOSED-LOOP CONTROL FACILITIES

A single hot-wire was connected to the hot-wire anemometers (Dantec Streamline), operating on a constant temperature circuit at an overheat ratio of 0.6, to measure the streamwise fluctuating velocity at x/D < 10. The voltage signal from the hot-wire was filtered at a cut-off frequency of 3 kHz, amplified 8 times and then digitized using a 16-bit A/D board (NI USB-6361) at a sampling frequency of 6 kHz. The sampling number of 480,000 (acquisition time is 80 sec) is used for the open-loop control experiments. The uncertainty of the hot-wire measurement has been estimated as less than 2%.

A NI USB-6361 system, connected to a personal computer, was used for closed-loop control study. The system contains 16 analog inputs (16 bit) and 2 analog outputs (16 bit) . The former

is used for acquiring the signal from hot wire as mentioned earlier and the latter is used for generating the control signal for minijet actuators at a rate of 6 kHz. The loop time is 0.4 seconds. The variation of f_e was realized by changing the frequency of the output square wave signal from the NI system output board. The Labview 2011 software was used to establish the link between the computer and the NI USB-6361 hardware. The interface for supervising information in real-time was designed with the Labview 2011 software.

FLOW VISUALIZATION SYSTEM

A planar PIV (Dantec SpeedSence90C10) system was deployed for flow visualization measurements in the injection (x, z) plane of the one minijet and the orthogonal non-injection (x, y) plane. A TSI oil droplet generator (TSI MCM-30) is used to generate fog for the seeding of flow. The particles are supplied into the mixing chamber (Figure 1a), which mix with air and fully spread throughout the main jet. Flow illumination was provided by two standard pulsed laser (Beam Tech 500-10) sources with 532 nm in wavelength and a maximum energy output of 120 mJ per pulse. Particle images were captured at a sampling rate of 10 Hz. The synchronization of flow illumination and image capturing was controlled by Dynamic studio v3.41. The captured images covered an area of x/D = 0 ~ 7 and y/D or z/D = - 3 ~ +5 in the (x, y) and (x, z) planes. The uncertainty of the position of the traversing system is about 0.1mm.

OPEN-LOOP CONTROL RESULS

The effect of the f_e on the K is firstly investigated at Re_D = 8000 and 9333 with a constant volumetric flow rate of the minijet, i.e. m = 2.5l/min. One objective of the open-loop control experiments is to provide the steady-state of input-output map between f_e and K in order to evaluate the feasibility of the closed-loop control. Figure 2(b) presents the measured K at different f_e for two different Reynolds numbers. At Re_D = 8000, the K strongly depends on f_e, showing a twin-peak value, with a global maximum (K = 0.425) at $f_e/f_0 \approx 0.5$ and the minor local maximum at $f_e/f_0 \approx 1.0$. The former is the optimal excitation frequency $f_{e,optimal}$ at Re_D = 8000 in this paper, leading to an increment in K by 818% compared with the natural jet. That is, $f_{e,optimal}$ is actually equal to one-half the frequency of the preferred-mode vortices. In order to illustrate the profound impact of control at $f_{e,optimal}$ on the main jet, we show typical photographs (Figure 3) in both injection (x, y) and non-injection (x, z) planes from flow visualization. There is a distinctly difference in the flow structure with and without control. Without control, the main jet remains laminar near the nozzle exit, as is evident in Figure 3. The potential core decrease significantly and the shear layer rollup occurs early under control and vortex paring occur early in both planes than the uncontrolled jet. The control result produces a vigorous entrainment of ambient fluid (dark-coloured around the vortex in the injection plane) into the jet. On the other hand, smoke-marked fluid (white-colored in the non-injection plane) is widely spread from the region where almost near the exit of the jet, producing an extensive diffusion than the uncontrolled case. When the Re_D is increase to 9333, the trends of the f_e/f_0-K curve are similar with that at Re_D of 8000. Note that, the K at Re_D of 9333 is less than that at Re_D of 8000, which is due to the C_m at Re_D of 9333 is smaller than that at Re_D of 8000.

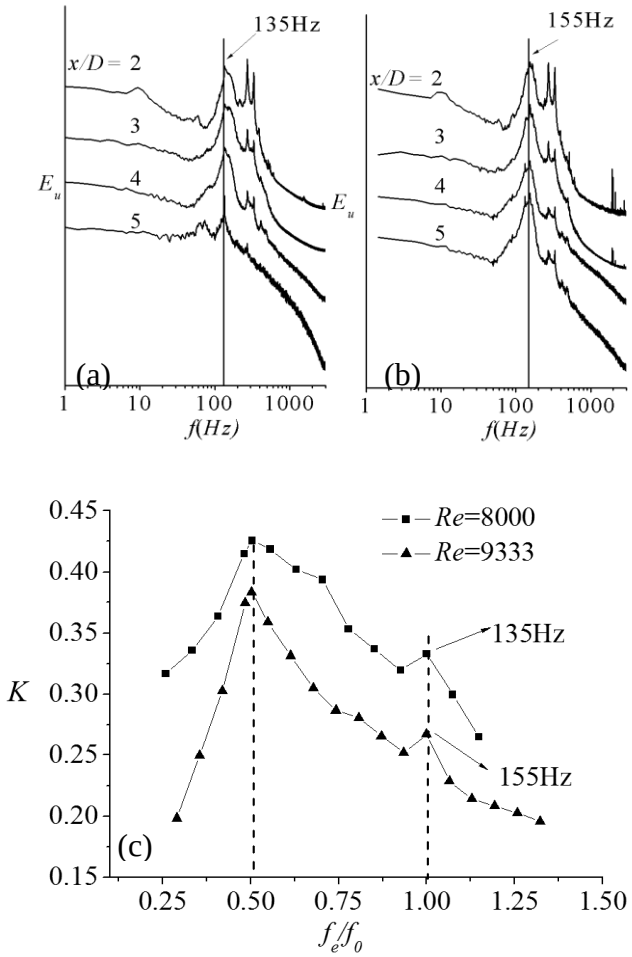

Figure 2 Power spectral density function of streamwise fluctuating velocity u measured on the centerline: (a) at Re_D = 8000; (b) at Re_D = 9333.
(c) The relationship of $K = F(f_e/f_0)$ for Re_D = 8000, 9333 for the open-loop control experiment.

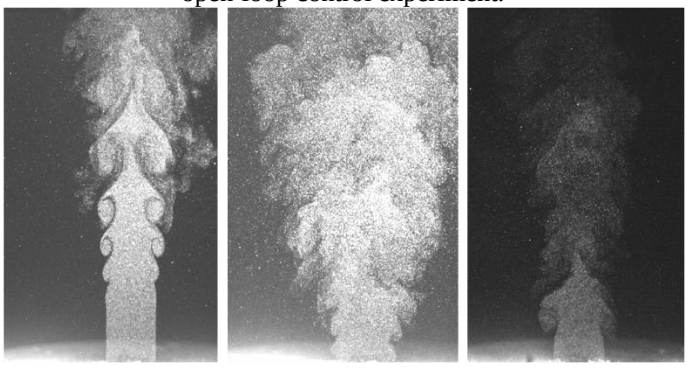

Figure 3 Photographs of flow visualization. Flow is from the bottom up at Re_D = 8000. Comparison in the typical flow structure (a) the uncontrolled jet and (b) the non-injection and (c) injection planes of controlled jet (C_m = 2.3%, f_e = 68 Hz), respectively.

CLASSICAL EXTREMUM SEEKING SCHEME

The schematic diagram of the classical extremum seeking algorithm is represented in Figure 4(a). The basic principle of the classic extremum seeking algorithm is given below. The flow control system is considered as a block with the input $f_e(t)$ and the output $<K>(t)$, where $< >$ indicates averaged quantity using 0.4-sec-long running window. A local maximum takes place on curve $<K> = F(f_e)$ when $f_e = f_{e,optimal}$, where the $d<K>/df_e = 0$. The algorithm drives the f_e automatically approaching $f_{e,optimal}$ following the feedback law, i.e., $df_e/dt = kd<K>/df_e$, where k is the gain and $d<K>/df_e$ is the local gradient of the input-output map. As such, autonomous adjustment of $f_e(t)$ from the initial excitation frequency $f_{e,i}$ to $f_{e,optiaml}$ is achieved

For calculating the $d<K>/df_e$, a small-amplitude sinusoidal signal $a\sin(\omega t)$ is superimposed on the control input f_e, i.e., $f_e(t) = f_{e,i} + \Delta f_e(t) + a\sin(\omega t)$, where ω $(=2\pi f_p)$ indicates the perturbation frequency and $\Delta f_e(t)$ is the feedback increment (Figure 4). This input can result in an approximate sinusoidal output in $<K>(t)$, fluctuating around the mean value $<K_{DC}>$ with the amplitude governed by aF'. That is, $<K>(t) = K_{DC} + aF'\sin(\omega t)$, where F' is the local gradient of the input-output curve. The $<K_{DC}>$ in the output is then removed by a first order high-pass filter (*HP*), i.e., $G_{HP}(j\omega) = j\omega/(j\omega+\omega_{HP})$, to produce $K_{HP}(t) = |G_{HP}|aF'$, where $|G_{HP}|$ is magnitude of the *HP* transfer function. The filtered signal $K_{HP}(t)$ is demodulated by multiplying a zero-mean signal with the perturbation $\sin(\omega t)$. The demodulated signal ξ $(= |G_{HP}|aF'\sin(\omega t))$ contains a constant, i.e., $|G_{HP}|(F'a/2)\cos(\phi_{HP})$, and a time-varying component, i.e., $|G_{HP}|$ $(F'a/2)\cos(2\omega t+\phi_{HP})$, where $|G_{HP}| = \frac{1}{\sqrt{1+(\omega_{HP}/\omega)^2}}$ and $\phi_{HP} = \arg(G_{HP}) = \arctan(\omega_{HP}/\omega)$. The time-varying component in y_d is then filtered out by a first order low-pass filter (*LP*). Thus, the output $K_{LP} = |G_{HP}|(F'a/2)\cos(\phi_{HP})$ is a steady signal proportional to the local gradient F'. The K_{LP} signal is then integrated and amplified by a gain k to obtain the feedback increment $\Delta f_e(t)$. In general, the $\Delta f_e(t)$ is positive for $f_e<f_{e,optimal}$, so the f_e would increase. Otherwise, f_e would decrease for $f_e>f_{e,optimal}$. Eventually, f_e will converge to $f_{e,optimal}$.

A NOVEL EXTREMUM SEEKING SCHEME

In classical extremum seeking scheme, the dynamic and static performance of the scheme is directly related to the amplitude a of the excitation sinusoidal signal $a\sin(\omega t)$. As the amplitude a increasing, the dynamic performance of the scheme becomes more effective and the static performance of the scheme becomes worse, and vice versa [13]. Therefore, on the basis of the classical methods, the novel extremum seeking scheme determine the amplitude a based on the variation of the estimated gradient, aiming to reduce the steady-state error [13].

As shown in Figure 4(b), the 'a' in the classical extremum seeking is replaced by a variable governed by $r\sqrt{|K_{LP}|}$ in the novel extremum seeking, i.e., $a = r\sqrt{|K_{LP}|}$, where the r is a constant factor. Since the $K_{LP} = |G_{HP}|(F'a/2)\cos(\phi_{HP})$ as discussed earlier in Figure 4(a), so we can get $a^2 = r^2|G_{HP}(F'a/2)\cos(\phi_{HP})|$. Therefore, the $a = |F'|r^2|G_{HP}\cos(\phi_{HP})/2|$, which indicates that the amplitude of the perturbation signal is proportional to the $|F'|$. Thus, the amplitude a will gradually reduce as the $|F'|$ approaches 0. In other words, the output fluctuation will decrease as the f_e converges to $f_{e,optimal}$.

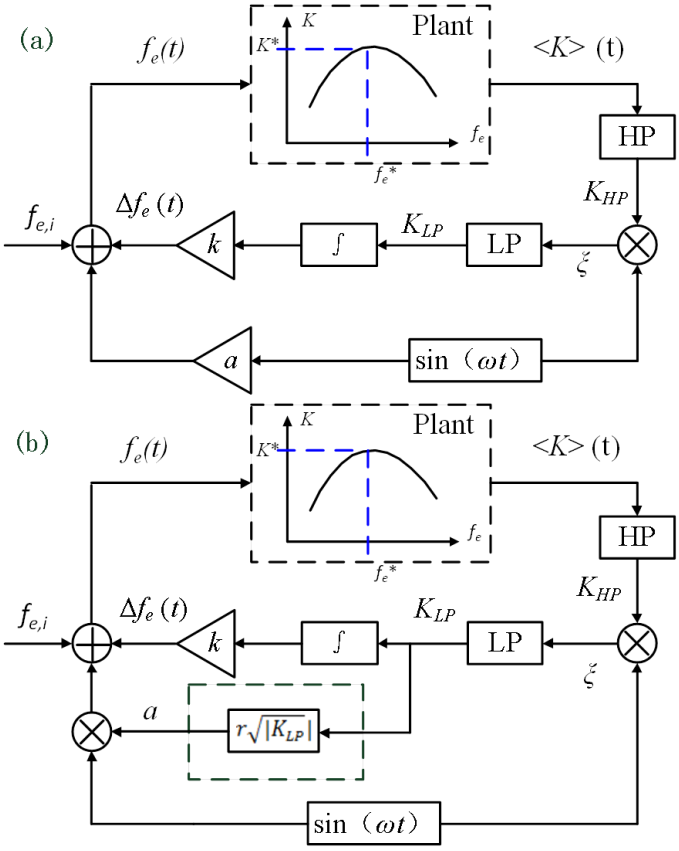

Figure 4 (a) Block diagram of the classical extremum seeking control scheme; (b) Block diagram of the novel extremum seeking control scheme.

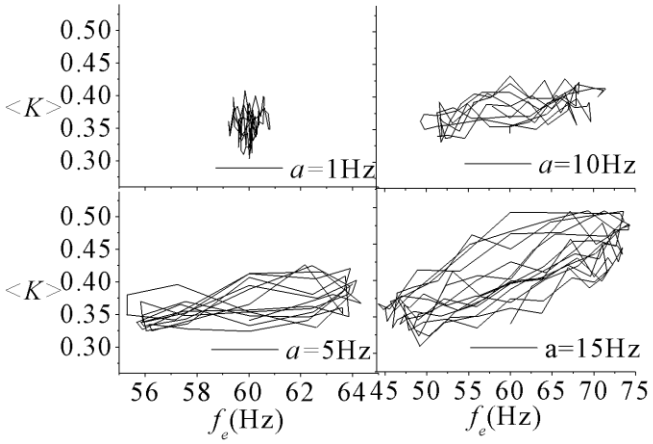

Figure 5 Effects of the amplitude a of the applied perturbation on the input–output map ($k = 0$, $Re_D = 8000$, perturbation imposed around $f_e = 60$ Hz).

IMPLEMENTATION AND PARAMETERIZATION OF THE NOVEL EXTREMUM SEEKING SCHEME

In most active flow control applications, the plant exhibits a hysteresis between the input and output signals, which may adversely affect the gradient estimation for the novel extremum seeking scheme. Using a sinusoidal input in the novel extremum seeking scheme may result in a phase shift of the output, however, appropriate setting of the perturbation parameters, i.e. f_p and a, of the controller could decrease the influence of hysteresis. The parameters of the ES controller are determined experimentally at Re_D = 8000 with the volumetric flow rate of one minijet fixed at C_m= 2.3%. The selection of key parameters in the control algorithm was similar to that used in [15]. A sinusoidal perturbation around the $f_{e,i}$ (= 60 Hz), i.e. $f_e(t) = f_{e,i} + a\sin(\omega t)$, is applied to the input signal to study the impact of different a and f_p on the K. Note that the k of 0 is used for the parameterization experiments. The amplitude a and f_p are investigated individually by fixing one of the two parameters and adjusting the other one. As such, we may determine the optimal perturbation parameters of the controller such that the output <K> is in phase with the $f_e(t)$. Figure 5 shows the comparison between the responses of <K> measured with a = 1, 5, 10 and 15 Hz (k = 0, Re_D = 8000, $f_{e,i}$ = 60 Hz, f_p = 0.125 Hz). The relation of <K> and f_e appears approximately a linear trend. At a = 1 Hz, the range of the sinusoidal perturbation yields a minor change in the <K> compared with that at a = 5 Hz, 10 Hz and 15 Hz, which means the amplitude a is too small. When a = 10 Hz and 15 Hz, the $f_e(t)$ could induce a conspicuous phase lag between <K> and f_e. As such, we choose a = 5 Hz， which is adequately large to influence the <K> signal but does not produce a significant hysteresis in the f_e-<K> map.

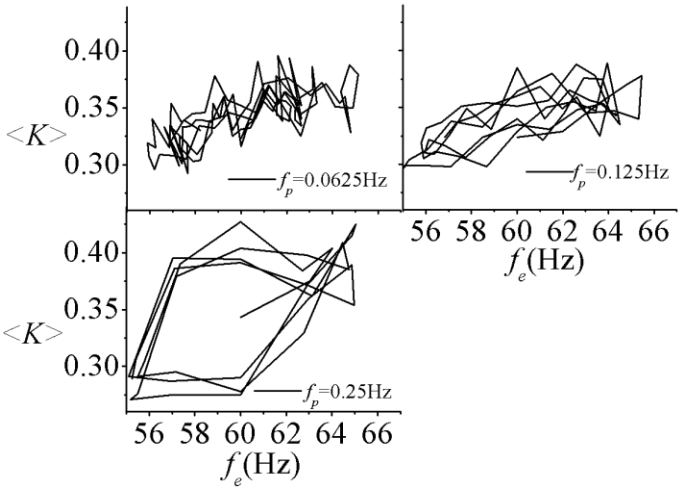

Figure 6 Effect of the frequency f_P of the applied perturbation on the input–output map (k = 0, Re_D = 8000, perturbation imposed around f_e = 60 Hz)

Figure 6 presents the response of <K> to the variation in f_p from 0.0625 Hz to 0.25 Hz. Firstly, the irregular changes in <K> occurs more obviously at f_p = 0.0625 Hz (Figure 6) compared with that at f_p= 0.125, 0.25 Hz. The reason may be due to the change in f_e is too slow at f_p = 0.0625 Hz. Thus, <K> is more easily disturbed by the external flow, adversely influencing the accurate gradient estimation. Secondly, the f_e-<K> map exhibits an extreme hysteresis at f_p = 0.25. Therefore, f_p = 0.125 Hz was selected for the controller, since only a small phase lag occurs in relationship between the f_e and <K> at f_p = 0.125 Hz. In addition, 0.1 times cutoff frequency is used for the *HP* and *LP* filters, i.e. $\omega_{HP} = \omega_{LP} = 0.1(2\pi f_p)$.

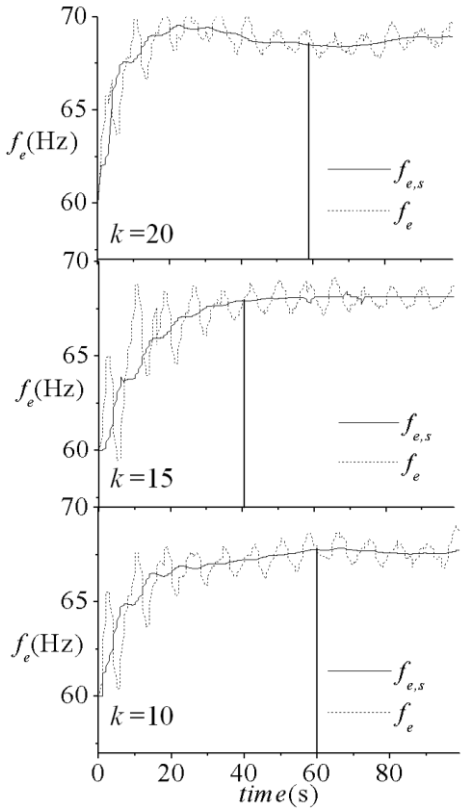

Figure 7 The f_e response of the controller at different gain k (Re_D = 8000, the feedback increment Δf_e is added t = 0 sec**)**

RESPONSE OF THE NOVEL EXTREMUM SEEKING SCHEME

Experiments are performed at Re_D = 8000 and C_m= 2.3% to investigate the performance of the novel extremum seeking algorithm not only in the search of the optimal f_e but also to choose the optimal gain k. Figure 7 presents the time domain response of the closed-loop control system for different gains k = 10, 15, 20, when a = 5 Hz, f_p = 0.125. Initially, the $f_{e,i}$ of 60 Hz is applied on the minijet at t = 0 sec, which is less than $f_{e,optimal}$ in the open-loop case (Figure 2(c)). The f_e increases immediately once the feedback signal is feedback to the controller at t > 0 sec. As indicated in Figure 7, the gain k has a direct impact on the feedback increment Δf_e, which may effect on the system stability and convergence time. For k = 10, it takes about 60 sec to converge the $f_{e,s}$ to near the $f_{e,optimal}$, where $f_{e,s} = f_{e,i} + \Delta f_e(t)$ is the quasi-steady component of f_e. As a result, the <K> converges to 0.41 after 60 sec. As the k increases, the change of Δf_e will be enlarged. Consequently, the convergence time reduces, about 40 sec, at k = 15. However, when the k

further increase to 20, the enlarged change in Δf_e may lead to an overshoot in f_e, thus increasing the fluctuation in <K> and weaken the system stability. In conclusion, k = 15 exhibits the shortest convergence time, and the good stability of the closed-loop control system.

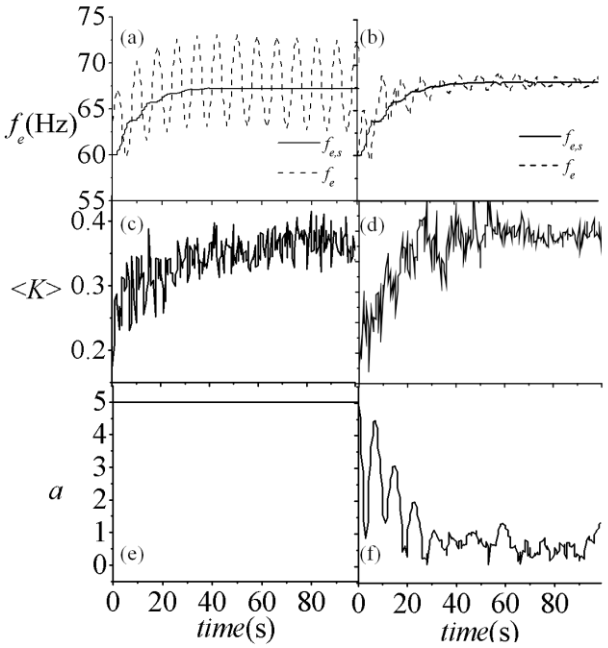

Figure 8 Compare the classical extremum seeking scheme and the novel extremum seeking scheme with f_e , <K> and a

For a better understanding of the novel extremum seeking scheme, we compared the results of the novel extremum seeking method with that of the classical one. As shown in Figure 8, the performance of the two methods show distinctly different under the same parameters, i.e. k = 15, $f_{e,i}$ = 60 Hz, f_p = 0.125 Hz and a = 5. For the classical extremum seeking scheme, the f_e gradually growth with a fixed perturbation amplitude due to the using of a fixed a = 5 Hz. After about 40 sec, the controller is stabilized with f_e fluctuating within 63-73 Hz (Figure 8a). Meanwhile, the K increases from 0.26 to 0.36 and is stabilized within 0.32 to 0.38 eventually (Figure 8c). On the other hand, the f_e in the novel extremum seeking begins with a large perturbation amplitude (Figure 8b). However, the perturbation amplitude decreases as the f_e approaching the $f_{e,optimal}$ and is stabilized at a range of 66.5 - 68.5 Hz. Correspondingly, the K increases from 0.26 to 0.40, stabilized within a range of 0.36 ~ 0.42 (Figure 8d). The reason is mainly due to the perturbation amplitude in the novel extremum seeking is $|F'|r^2|G_{HP}\cos(\phi_{HP})/2|$, which is directly proportional to $|F'|$ since the value of r, G_{HP}, $\cos(\phi_{HP})$ are constant. The $|F'|$ tends to zero as time in the novel extremum seeking. Thus the amplitude a also tends to zero as shown in Figure 8 (f), however, the amplitude a in the classical extremum seeking is a constant (Figure 8e). Therefore, the amplitude a of the novel scheme will less than the amplitude a of the classical scheme when the control schemes are stable. Accordingly, the change of a in the novel scheme could lead to a reduction in the steady-state error of f_e by 80%. More importantly, the mean value of the stabilized <K> increased by 11.11% compared classical scheme (from 0.36 to 0.40). The mean value of the stabilized <K> is averaged from the 40 to 100 sec corresponding to the <K> in Figure 8c and 8d.

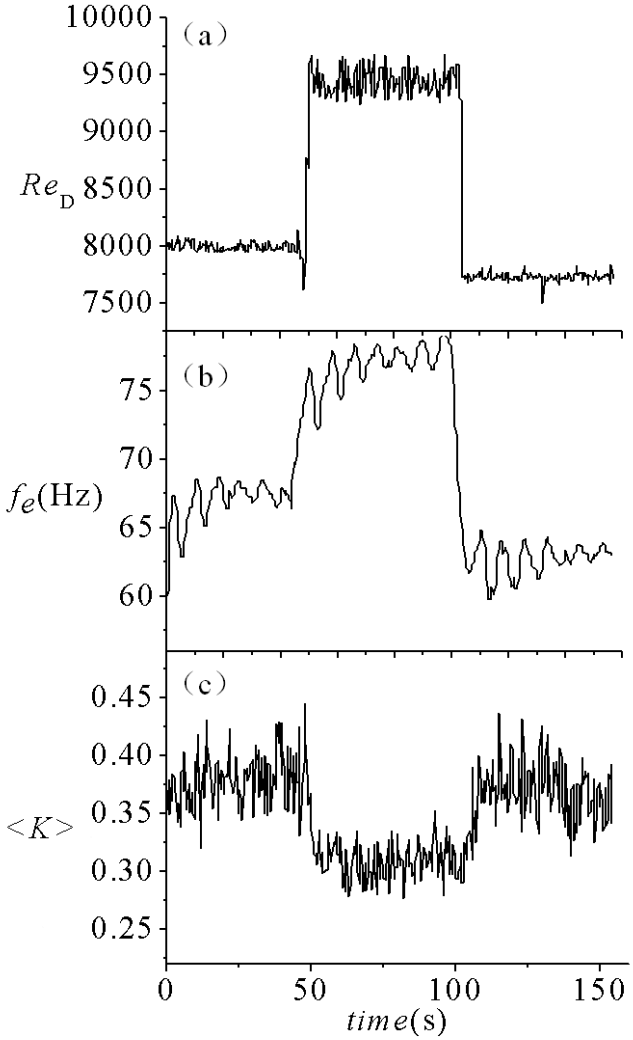

Figure 9 Responses of the novel extremum seeking scheme to varying Re_D: (1) from Re_D= 8000 to 9600 at 45 sec. (2) from Re_D= 9600 to 7333 at 104 sec, C_m=2.3%

Robustness is an important aspect for a closed-loop control system and is one of the important indicators for the overall control performance. The robustness is examined when Re_D is changed suddenly at a fixed C_m and k = 15. At Re_D = 8000, the controller is applied at t = 0 sec and the control system takes about 40 sec to increase f_e from $f_{e,i}$ to $f_{e,optimal}$ = 67.5 Hz (Figure 9b). The <K> signal increases from around 0.015 to 0.40 accordingly (Figure 9c). The results are consistent with that achieved in Figure 8, indicating a good repeatability of the control system. As Re_D is suddenly increased from 8000 to 9600 at t = 45 sec (Figure 9a), the f_e-K map changes and $f_{e,optimal}$ rises. The gradient of the f_e-<K> curve becomes positive, resulting in a positive Δf_e. The controller increases f_e until the maximum <K> is reached, with $f_{e,optimal}$ = 78Hz. Note that

$f_{e,optimal}$ = 78 Hz is slightly higher than the optimal f_e (= 77.5 Hz) achieved at Re_D = 9600, due to a slightly higher Re_D. On the other hand, as Re_D is decreased from 9600 to 7333 at 104 sec, the controller could also maintain a stable f_e at $f_{e,optimal}$ and <*K*> = 0.38 (Figure 9c), indicating an excellent robustness. The adaptation of the controller is studied by applying two different initial excitation frequencies, i.e., $f_{e,i}$ = 60 Hz and 75 Hz, at Re_D = 8000. When $f_{e,i}$ is less than $f_{e,optimal}$ (= 67.5 Hz), the gradient of the f_e-<*K*> curve (Figure 2) is positive, corresponding to a positive Δf_e. On the other hand, when $f_{e,i}$ is larger than $f_{e,optimal}$, the gradient is negative; so is Δf_e. As shown in Figure 10, in all the cases, the controller adjusts f_e [= $f_{e,i}(t) + \Delta f_e\ (t) + a\sin(\omega t)$] to $f_{e,optimal}$, where the gradient of the f_e-<*K*> curve is zero, suggesting an excellent adaptation.

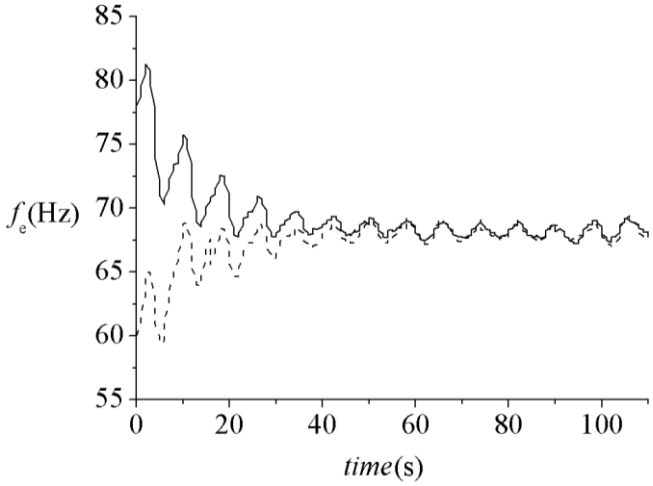

Figure 10 The f_e response of the novel extremum seeking scheme at different $f_{e,i}$

CONCLUSION

The closed-loop control of a turbulent round jet has been experimentally investigated based on a single unsteady radial minijet.

1. The open-loop control, with C_m fixed at 2.3%, is highly effective in enhancing the jet mixing performance at Re_D = 8000, producing an increase in *K* by 818% at $f_{e,optimal}$ = $0.5f_0$, compared with the natural jet. Accordingly, the flow structure exhibits a drastic change.
2. The novel extremum seeking feedback control has been developed without *a* priori knowledge of relevant fluid dynamics. The system output <*K*> is obtained online. Given a fixed C_m, the novel extremum seeking controller succeeds in finding autonomously $f_{e,optimal}$ and hence the maximum <*K*>, as obtained in the open-loop control. This control technique is also found to be robust and adaptable when Re_D and $f_{e,i}$ are separately changed. More importantly, the novel scheme can reduce the steady-state error of f_e by 80% and meanwhile increase the mean <*K*> by 11%, compared with the classical scheme. The choice of the parameters in the controller is crucial for the desired control performance. The right amplitude *a* and frequency f_p of the applied sinusoidal perturbation may lead to a minimum phase lag between the input and output signal, thus ensuring accurate gradient estimation. On the other hand, the proper selection of gain *k* may promote the stability of the system.

ACKNOWLEDGEMENT

Authors wish to acknowledge support from National Natural Science Foundation of China (Grant Nos 11402068 and 51275550).

REFERENCES

[1] Bradbury L J S, Khadem A H. The distortion of a jet by tabs. *Journal of Fluid Mechanics*, 1975, 70:801-813.
[2] Zaman K B M Q. Spreading Characteristics of Compressible Jets from Nozzles of Various Geometries. *Journal of Fluid Mechanics*, 1999, 383(6):197-228.
[3] Mi J, Nathan G J, Luxton R E. Centreline mixing characteristics of jets from nine differently shaped nozzles. *Experiments in Fluids*, 2000, 28(1):93-94.
[4] Davis M R. Variable control of jet decay. *AIAA Journal*, 1982, 20(20):606-609.
[5] Ginevsky A S, Vlasov Y V, Karavosov R K. *Acoustic Control of Turbulent Jets*. Springer Berlin Heidelberg, 2004.
[6] Glezer A, Amitay M. Synthetic jets. *Annual Review of Fluid Mechanics*, 2002, 34(1):503-529.
[7] Corke T C, Enloe C L, Wilkinson S P. Dielectric Barrier Discharge Plasma Actuators for Flow Control. *Annual Review of Fluid Mechanics*, 2009, 42(1):505-529.
[8] Zhou Y, Du C, Mi J, et al. Turbulent Round Jet Control Using Two Steady Minijets. *AIAA Journal*, 2012, 50(3):736-740.
[9] Freund J B, Moin P. Jet Mixing Enhancement By High Amplitude Fluidic Actuation. *AIAA Journal*, 2000, 38(10):1863-1870.
[10] Zhang M M, Cheng L, Zhou Y. Closed-loop control of fluid–structure interactions on a flexibly supported cylinder. *European Journal of Mechanics - B/Fluids*, 2004, 23(1):189-197.
[11] Ariyur K B, Krstic M. Real-Time Optimization by Extremum Seeking Control// Real time optimization by extremum seeking control. *John Wiley*, 2003:xii,236
[12] Benard N, Moreau E, Griffin J, et al. Slope seeking for autonomous lift improvement by plasma surface discharge. *Experiments in Fluids*, 2010, 48(5):791-808.
[13] Wang L, Chen S, Zhao H. A novel fast extremum seeking scheme without steady-state oscillation// Control Conference (CCC), 2014 33rd Chinese. IEEE,2014.
[14] Mi J, Nobes D S, Nathan G J. Influence of jet exit conditions on the passive scalar field of an axisymmetric free jet. J Fluid Mech. *Journal of Fluid Mechanics*, 2001, 432(7):91-125.
[15] Maury R, Koenig M, Cattafesta L, et al. Extremum-seeking control of jet noise. *International Journal of Aeroacoustics*, 2012, 11(3):459-474.